Supporting Information

Delicate Crystallinity Control Enables High-Efficiency P3HT Organic Photovoltaic Cells

Kaihu Xian, Yang Liu, Junwei Liu, Jinde Yu, Yifan Xing, Zhongxiang Peng, Kangkang Zhou, Mengyuan Gao, Wenchao Zhao, Guanghao Lu, Jidong Zhang, Jianhui Hou, Yanhou Geng and Long Ye*

Instruments and Measurements

Electrochemical Properties. The *J-V* measurements were performed via the AAA solar simulator (SS-F5-3A, Enli Technology Co. Ltd, Taiwan) along with AM 1.5G spectra whose intensity was calibrated by the certified standard silicon solar cell at 100 mW/cm^2. The EQE spectra were measured through the Solar Cell Spectral Response Measurement System QE-R3011 (Enli Technology Co. Ltd, Taiwan). The thickness of blend layers was measured via the surface profilometer Bruker Dektak XT.

GIWAXS Characterizations. The samples for GIWAXS measurements were prepared on silicon substrates and the conditions were the same as the device preparation. GIWAXS experiments were carried out at BL14B1 beamline of Shanghai Synchrotron Radiation Facility (SSRF). The X-ray energy was 10 keV, corresponding to the wavelength of 1.24 Å. The incidence angle was 0.2° and the sample-to-detector distance was 357 mm by careful calibration. The beam center and sample-to-detector distance were calibrated with LaB_6. GIWAXS characterizations were also carried out at the beamline 1W1A of Beijing Synchrotron Radiation Facility (BSRF).

Morphology Characterizations. The surface microtopography of films was measured by a Nanoscope V AFM (Bruker Multimode 8) in tapping mode. The type of AFM cantilever is RTESPA-300 with a *k* constant of about 40 N/m. The scanning area was 2 μm × 2 μm and the resolution is 256∗256 pixels. The TEM images of films were obtained by the JEOL JEM-2100PLUS electron microscope and its accelerating voltage is 200 kV. The magnification of all neat P3HT and blend TEM images is 30 k and neat ZY-4Cl is 10 k.

Optical Absorption and Charge Transport Properties. Absorption spectra of all of the materials in the solutions and in the solid thin films were measured on Shimadzu UV3600 plus spectrometer. Solution spectra were measured in THF and thin-films were prepared by spin coating from their THF solutions. The hole and electron mobilities were measured by the SCLC method, employing device architectures of ITO/PEDOT:PSS/P3HT:ZY-4Cl/MoO_3/Al and ITO/ZnO/P3HT:ZY-4Cl/Al, respectively. The mobilities were obtained by taking the dark current-voltage curves in the range 0-7 V and fitting the results to a space charge limited form. The equation $J = (9/8)\varepsilon_0\varepsilon\mu_0 V^2/L^3 exp(0.89\sqrt{V/E_0 L})$ was used to calculate the hole mobilities. where J is the current density, ε_o is the vacuum permittivity, ε is the relative permittivity of the organic donor material, μ is the charge carrier mobility, V is the effective applied voltage, L is the thickness of the film. And the equation $J = (9/8)\varepsilon_0\varepsilon_r\mu_e V^2/L^3$ was used to calculate the electron mobilities, where ε_r is the relative permittivity of the organic acceptor material, μ is the charge carrier mobility.

Dynamic Mechanical Analysis: A TA Q800 DMA was used to perform DMA measurements. Polymer solutions (15 mg mL^{-1}) were made and the sample were prepared by drop-casting polymer solutions onto a glass fiber mesh. The temperature corresponding to the peak of tan δ was determined as the backbone T_g. In strain-controlled mode, temperature ramp experiments were performed at a temperature range of -50 to 100 ℃ and a heating rate of 3 ℃ min^{-1} with a fixed frequency of 1 Hz. The strain imposed was in the linear regime.

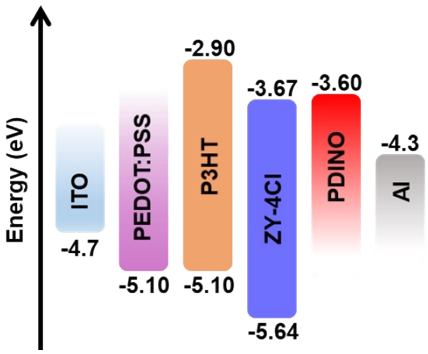

Figure S1. Molecular energy level alignments in this work.

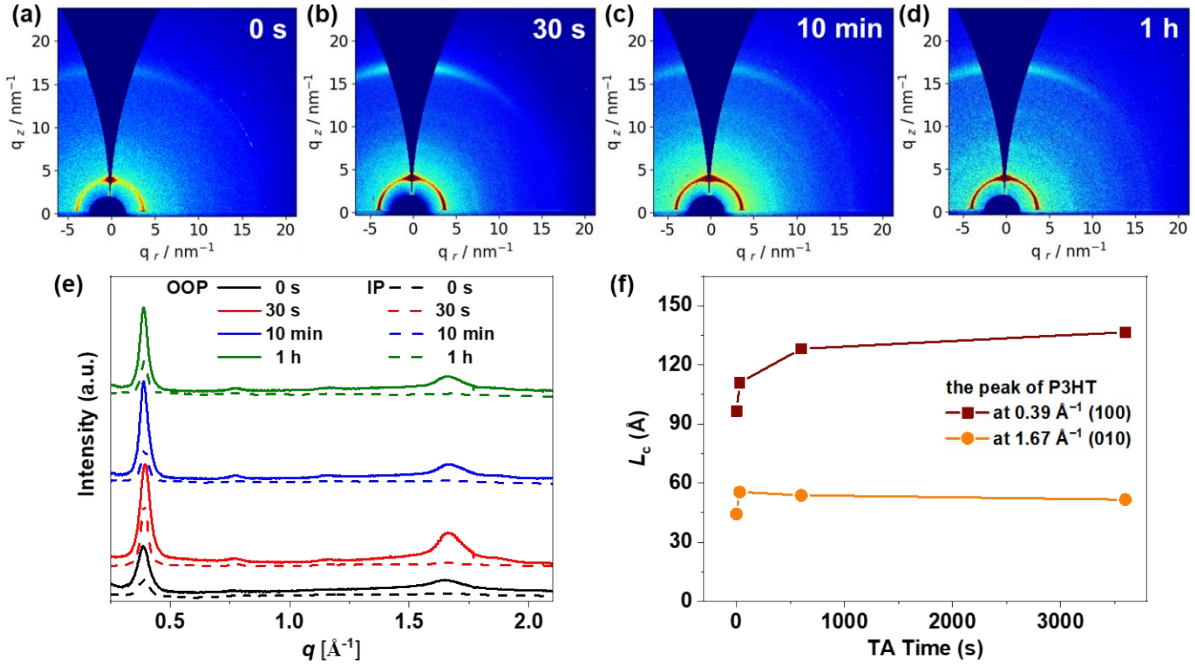

Figure S2. (a-d) The time-dependent evolution of 2D GIWAXS patterns of the neat P3HT films with annealing time. (e) The corresponding out-of-plane and in-plane sector-averaged profiles for the films. (f) The corresponding L_c plots of (100) and (010) reflection.

Table S1. The (100), (200), (300) and (010) peak position and L_c of neat P3HT films annealing for different time.

Sample	Position (Å^{-1})	Stacking Distance (Å)	FWHM (Å^{-1})	L_c (Å)
0 s	0.39	16.17	0.06	96.57
	0.77	8.14	0.07	75.93
	1.15	5.46	0.07	81.46
	1.65	3.80	0.13	44.33
30 s	0.39	15.91	0.05	111.01
	0.77	8.11	0.07	85.62
	1.16	5.42	0.10	58.22
	1.67	3.77	0.10	55.52
10 min	0.39	16.09	0.04	128.23
	0.77	8.13	0.06	88.07
	1.16	5.42	0.08	66.90
	1.67	3.76	0.11	53.84

1 h	0.39	16.13	0.04	136.61
	0.77	8.11	0.07	78.10
	1.16	5.42	0.08	71.91
	1.67	3.77	0.11	51.69

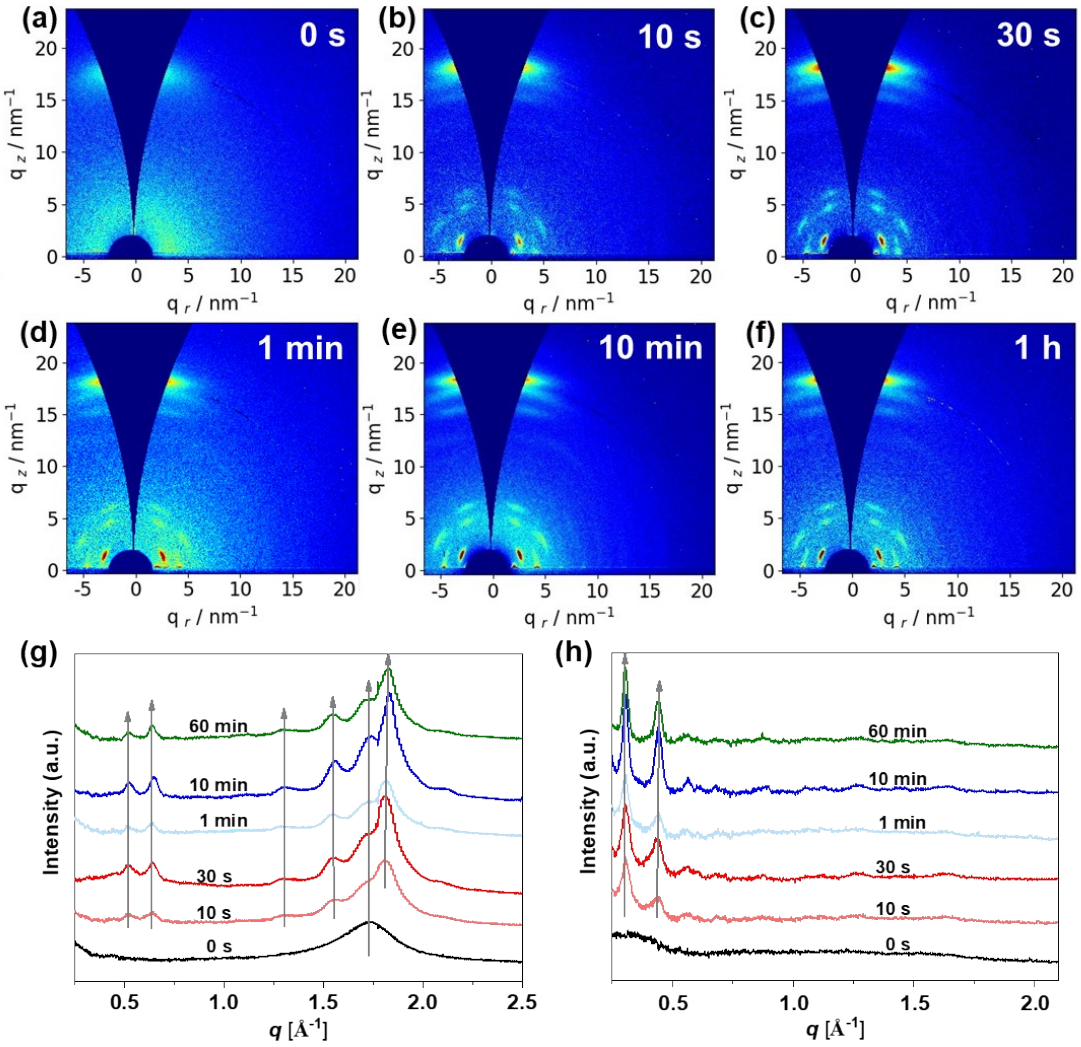

Figure S3. (a-f) The time-dependent evolution of 2D GIWAXS patterns of the neat ZY-4Cl films with annealing time. The corresponding (g) out-of-plane and (h) in-plane sector-averaged profiles for the films.

Table S2. The peak position and L_c of different peaks of neat ZY-4Cl films annealing for different time.

Sample	Position (Å^{-1})	Stacking Distance (Å)	FWHM (Å^{-1})	L_c (Å)
0 s	1.72	3.66	0.36	15.72
10 s	0.52	12.06	0.08	71.20
	0.64	9.89	0.05	117.36
	1.33	4.71	0.22	25.30
	1.56	4.04	0.14	40.13
	1.68	3.73	0.09	64.90
	1.81	3.48	0.18	31.29

30 s	0.52	12.12	0.19	29.90
	0.64	9.79	0.05	110.70
	1.33	4.73	0.16	35.63
	1.55	4.04	0.14	40.75
	1.69	3.72	0.08	67.17
	1.81	3.47	0.15	38.45
1 min	0.52	12.09	0.05	124.02
	0.63	9.90	0.05	121.20
	1.32	4.75	0.19	29.27
	1.55	4.05	0.13	43.33
	1.69	3.72	0.08	67.57
	1.81	3.46	0.14	39.34
10 min	0.52	12.01	0.05	116.30
	0.65	9.73	0.05	116.04
	1.31	4.80	0.11	51.95
	1.55	4.04	0.10	57.66
	1.71	3.67	0.11	53.38
	1.83	3.43	0.12	46.72
1 h	0.52	12.04	0.05	110.96
	0.64	9.84	0.04	142.42
	1.33	4.73	0.16	34.34
	1.55	4.06	0.12	48.30
	1.70	3.71	0.09	62.14
	1.82	3.45	0.13	42.48

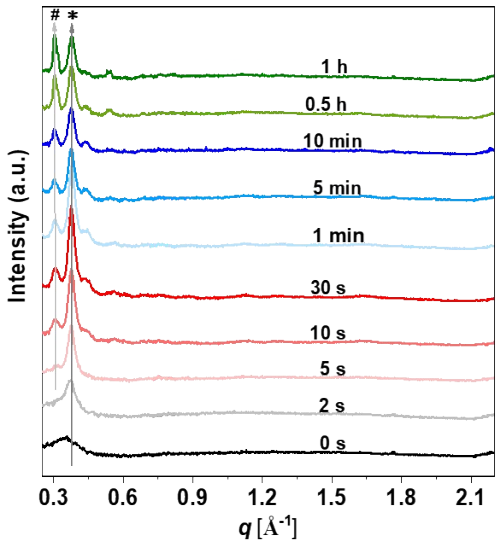

Figure S4. The corresponding in-plane sector-averaged profiles for all of the blend films.

Table S3. The peak position and L_c of different peaks of out-of-plane sector-averaged profiles for all blend films annealing for different time.

Sample	Position (Å^{-1})	Stacking Distance (Å)	FWHM (Å^{-1})	L_c (Å)
0 s	1.67	3.77	0.34	16.75
2 s	0.38	16.47	0.05	109.09
	1.67	3.76	0.29	19.71

5 s	0.39	15.97	0.06	100.39
	0.62	10.07	0.03	165.89
	1.69	3.72	0.25	22.81
	1.83	3.44	0.11	49.92
10 s	0.40	15.78	0.05	104.10
	0.52	12.18	0.10	55.35
	0.64	9.85	0.05	107.25
	1.31	4.80	0.16	36.12
	1.68	3.75	0.11	49.73
	1.81	3.47	0.10	57.74
30 s	0.40	15.79	0.06	97.25
	0.52	12.12	0.09	64.73
	0.64	9.86	0.05	117.47
	1.33	4.72	0.20	28.36
	1.53	4.10	0.11	53.19
	1.68	3.75	0.13	42.40
	1.81	3.47	0.12	48.33
1 min	0.40	15.79	0.05	109.07
	0.52	12.10	0.07	80.43
	0.64	9.86	0.05	120.05
	1.35	4.65	0.32	17.66
	1.54	4.09	0.08	66.57
	1.68	3.74	0.15	38.23
	1.82	3.46	0.14	39.31
5 min	0.39	16.11	0.03	163.09
	0.51	12.25	0.05	108.36
	0.63	9.96	0.03	165.14
	1.35	4.65	0.35	16.00
	1.53	4.12	0.88	6.44
	1.67	3.76	0.13	41.98
	1.81	3.48	0.11	51.30
10 min	0.39	16.17	0.03	183.69
	0.53	11.89	0.07	80.01
	0.63	9.97	0.03	193.81
	1.32	4.76	0.54	10.43
	1.52	4.12	0.10	58.37
	1.67	3.76	0.13	43.73
	1.81	3.48	0.10	54.84
0.5 h	0.39	16.23	0.04	131.93
	0.50	12.44	0.03	204.32
	0.56	11.20	0.02	229.42
	0.63	9.91	0.04	131.74
	1.33	4.72	0.27	20.74
	1.49	4.21	0.13	44.53
	1.67	3.76	0.16	35.09
	1.82	3.45	0.11	49.43
1 h	0.31	20.46	0.02	291.61
	0.39	16.27	0.05	117.92
	0.50	12.49	0.02	252.70
	0.56	11.24	0.02	269.46
	0.63	9.92	0.04	141.06

0.76	8.26	0.10	57.03
1.34	4.69	0.21	26.60
1.48	4.24	0.13	42.05
1.67	3.77	0.16	35.83
1.82	3.45	0.09	59.96

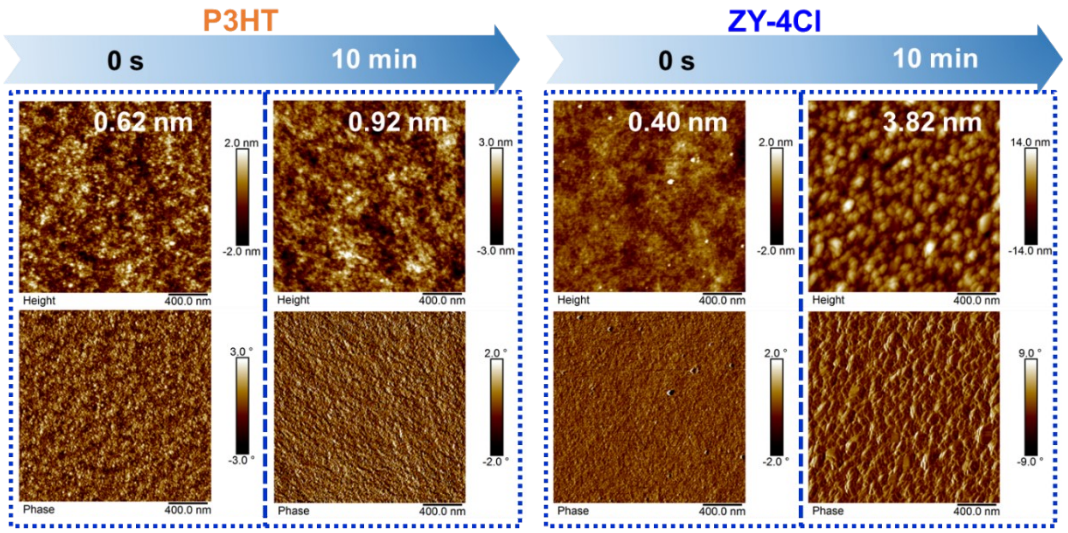

Figure S5. The AFM height and phase images of as-cast and 10 min annealed neat films.

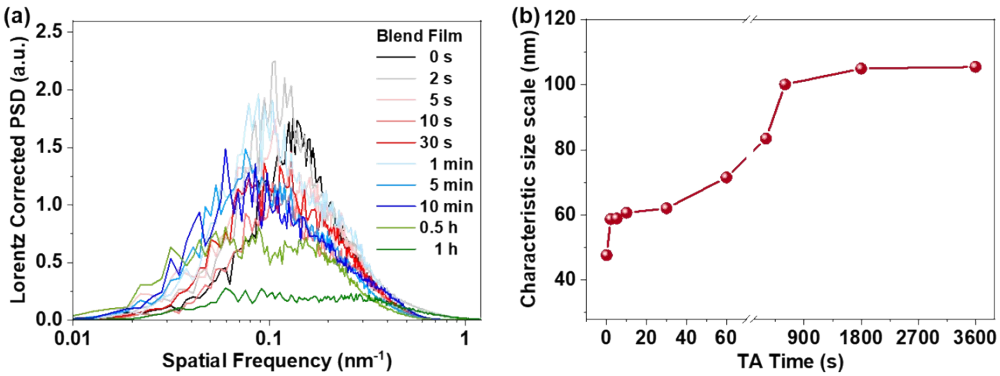

Figure S6. (a) PSD profiles of the AFM phase images for the blend films. The scale bars are inserted in the AFM images. (b) The evolution plot of the characteristic size scale calculated from PSD profiles with annealing time.

Table S4. The Characteristic size scales of the blend films with annealing time.

Time	0 s	2 s	5 s	10 s	30 s	1 min	5 min	10 min	0.5 h	1 h
Characteristic size scale (nm)	47.6	58.7	58.9	60.7	62.0	71.5	83.4	100.0	104.9	105.4

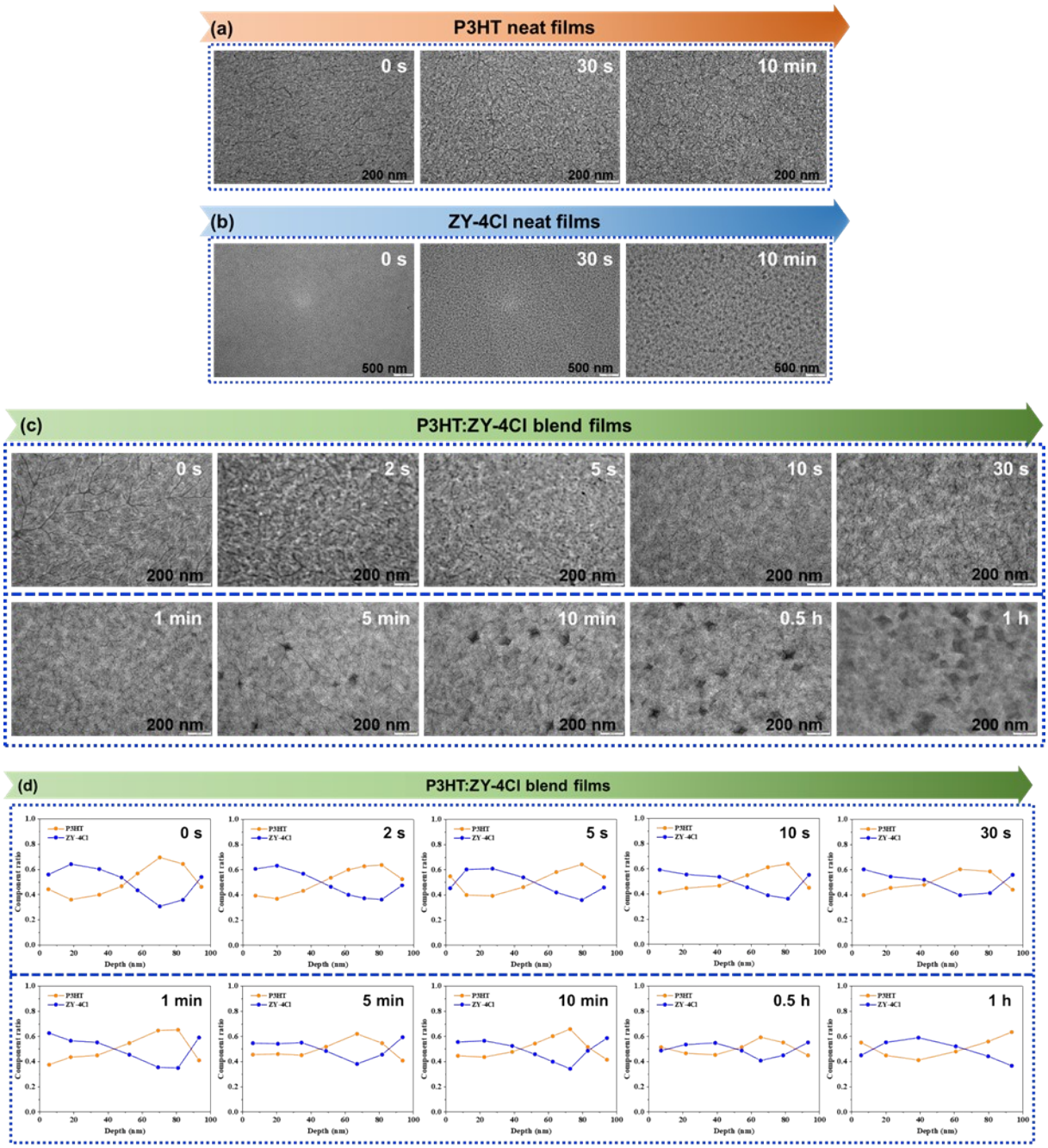

Figure S7. The evolution of TEM images of (a) neat P3HT, (b) neat ZY-4Cl and (c) blend films with annealing time. (d) The vertical profiles of each component across the whole thickness of the active layers, measured by *in situ* film-depth-dependent light absorption spectroscopy (FLAS) technique.

Table S5. The detailed absorption coefficients at ~560 (P3HT) and 700 nm (ZY-4Cl) of the blend films with annealing time.

Material	Time	0 s	2 s	5 s	10 s	30 s	1 min	5 min	10 min	0.5 h	1 h
P3HT	wave length (nm)	542	542	545	554	560	560	560	560	560	560
	ε (10^5/cm)	0.812	0.822	0.894	0.88	0.888	0.858	0.868	0.882	0.886	0.886
	wave	688	689	691	697	700	700	700	700	701	702

ZY-4Cl	length (nm) ε (10^5/cm)	0.692	0.698	0.736	0.792	0.81	0.778	0.778	0.782	0.758	0.714

Table S6. The detailed P_{diss} of the devices with annealing time.

Heating Time	0 s	2 s	5 s	10 s	30 s	1 min	5 min	10 min	0.5 h	1 h
P_{diss} (%)	11.9	13.3	53.0	89.7	94.6	93.9	95.9	95.6	96.7	91.6

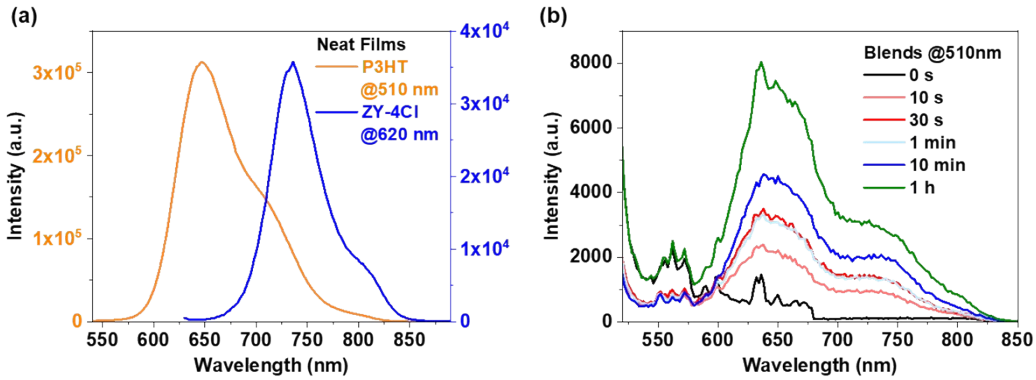

Figure S8. PL spectra of (a) neat P3HT (excited at 510 nm) and neat ZY-4Cl (excited at 620 nm). (b) PL spectra of P3HT:ZY-4Cl blend films (excited at 510 nm).

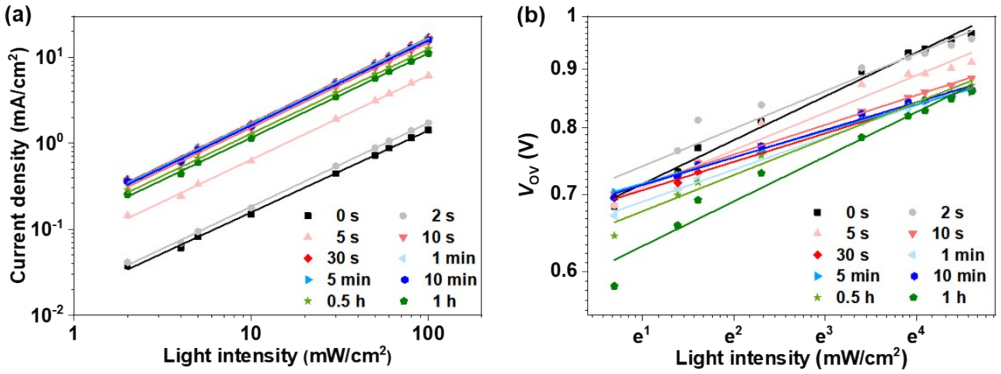

Figure S9. The extracted plots of (a) J_{SC} and (b) V_{OC} versus light intensity for the optimized devices.

Table S7. The detailed α and β of the devices with annealing time.

Time	0 s	2 s	5 s	10 s	30 s	1 min	5 min	10 min	0.5 h	1 h
α	0.952	0.975	0.979	0.988	0.989	0.989	0.988	0.986	0.982	0.983
β (kT/e)	1.97	1.76	1.78	1.51	1.47	1.49	1.39	1.43	1.74	1.91

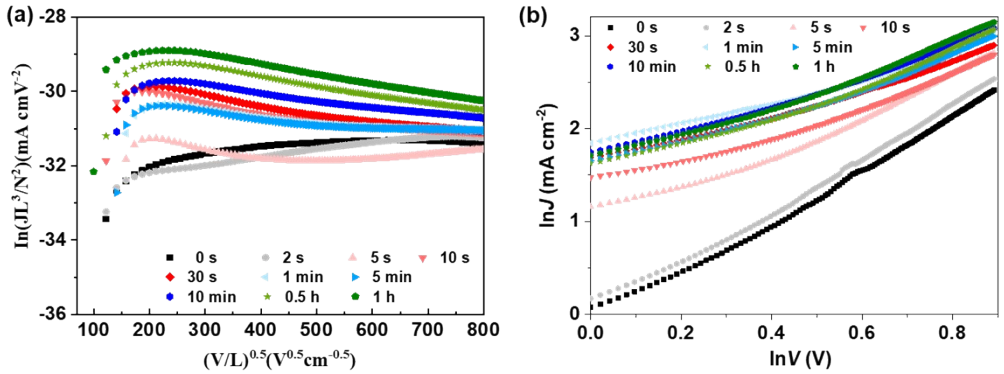

Figure S10. The (a) hole and (b) electron mobilities measured by SCLC method.

Table S8. The detailed hole mobility, electron mobility and μ_e/μ_e of the devices with annealing time.

Heating Time	0 s	2 s	5 s	10 s	30 s	1 min	5 min	10 min	0.5 h	1 h
Hole ($\times10^{-4}$ cm^2 V^{-1}s^{-1})	0.39	0.29	0.68	2.25	3.36	3.98	4.96	8.10	10.4	19.1
Electron ($\times10^{-4}$ cm^2 V^{-1}s^{-1})	0.36	0.40	1.06	1.48	1.81	2.10	1.76	1.83	1.69	1.65
μ_e/μ_e	1.1	0.7	0.6	1.5	1.9	1.9	2.8	4.4	6.2	11.6

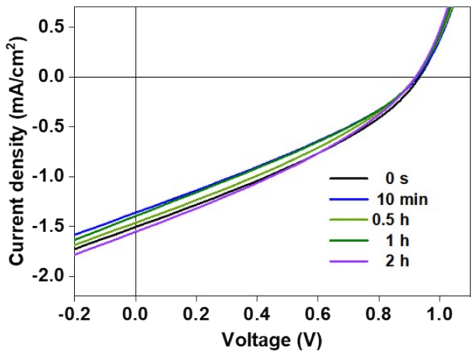

Figure S11. *J-V* curves of the as-cast P3HT:ZY-4Cl films under high vacuum (10^{-4} Pa) for different times to eliminate the residual solvent effect.

Table S9. Detailed photovoltaic parameters of the as-cast P3HT:ZY-4Cl films under high vacuum for different times.

Time	V_{OC} (V)	J_{SC} (mA/cm^2)	FF (%)	PCE (%)
0 s	0.974	1.51	33.0	0.485
10 min	0.967	1.36	31.0	0.408
0.5 h	0.962	1.46	31.9	0.449
1 h	0.963	1.40	30.8	0.415
2 h	0.961	1.55	32.6	0.486

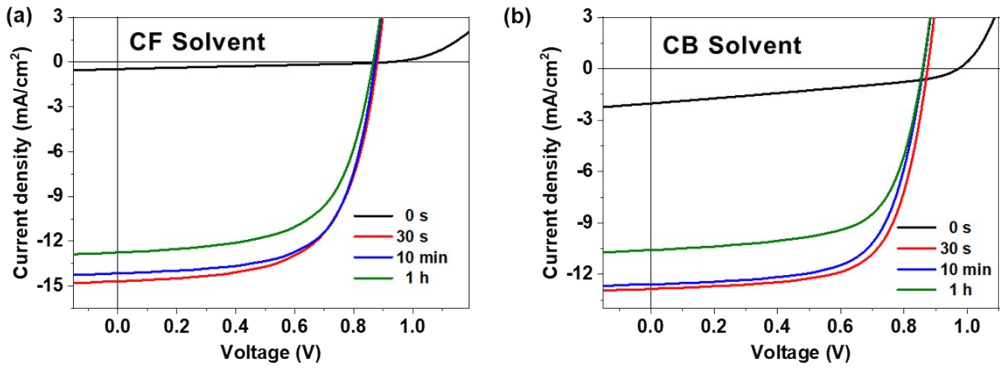

Figure S12. *J-V* curves of the optimal P3HT:ZY-4Cl blend films with different annealing times with (a) CF and (b) CB as processing solvents.

Table S10. Detailed photovoltaic parameters of the P3HT:ZY-4Cl films with different annealing times with (a) CF and (b) CB as processing solvents.

Solvent	Time	V_{OC} (V)	J_{SC} (mA/cm^2)	FF (%)	PCE (%)
CF	0 s	0.918	0.47	27.4	0.12
	30 s	0.880	14.68	62.5	8.07
	10 min	0.873	14.12	64.3	7.93
	1 h	0.866	12.75	61.7	6.81
CB	0 s	0.975	2.03	33.9	0.67
	30 s	0.874	12.86	67.4	7.58
	10 min	0.861	12.60	66.4	7.20
	1 h	0.858	10.59	65.7	5.97

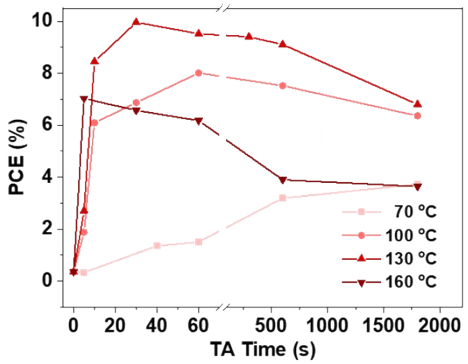

Figure S13. The evolution plots of PCE at different TA temperatures with annealing time.

Table 11. Detailed photovoltaic parameters of the P3HT-OPV cells as a function of annealing time at different TA temperatures under AM 1.5 G illumination.

Temperature (°C)	Time	V_{OC} (V)	J_{SC} (mA/cm^2)	FF (%)	PCE (%)
/	0 s	0.974	1.18	31.7	0.36
70	5 s	0.927	1.20	30.9	0.34
	40 s	0.947	3.70	38.7	1.36
	1 min	0.937	4.06	39.6	1.51
	10 min	0.927	7.06	48.8	3.19
	30 min	0.913	7.72	52.9	3.73
100	5 s	0.914	5.14	39.9	1.88
	10 s	0.897	10.81	62.8	6.09
	30 s	0.859	14.04	57.0	6.87
	1 min	0.872	14.45	63.5	8.01
	10 min	0.856	14.39	61.1	7.52
	30 m in	0.841	12.89	58.6	6.36
130	5 s	0.921	6.09	48.4	2.71
	10 s	0.900	14.89	63.1	8.45
	30 s	0.896	16.28	68.3	9.96
	1 min	0.894	16.27	65.4	9.52
	5 min	0.880	16.42	65.0	9.40
	10 min	0.878	16.35	63.5	9.11
	30 min	0.869	11.79	66.3	6.80
160	5 s	0.877	12.56	63.8	7.03
	30 s	0.845	12.03	64.7	6.57
	1 min	0.835	11.44	74.7	6.18
	10 min	0.778	7.90	63.5	3.90
	30 min	0.754	7.41	65.1	3.64

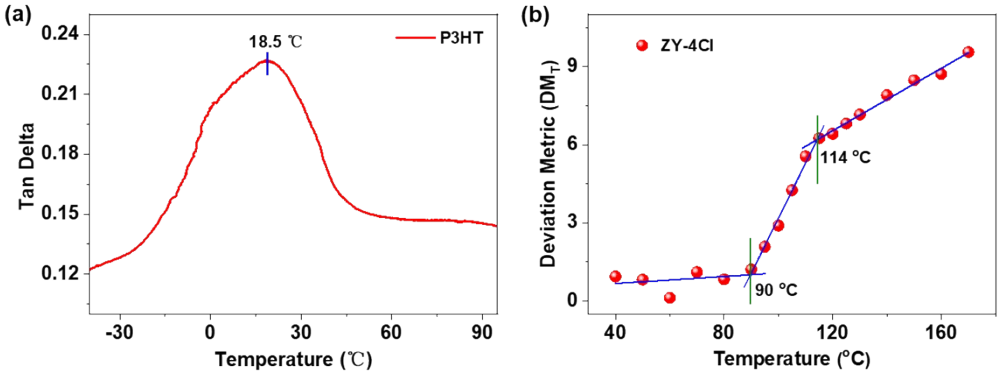

Figure S14. (a) Dynamic mechanical analysis curve of P3HT. The peak of tanδ versus T can be assigned to the T_g of P3HT. (b) Evolution of the deviation metric as a function of annealing temperature of ZY-4Cl, showing a distinct increase at the low T transition (~90 °C). The procedures were detailed in a prior study (S. E. Root *et al.*, *Chem. Mater.* **2017**, *29*, 2646-2654).